Vol. 7, No. 4, August 2023, pp. 345-353

Current Optics and Photonics

Regular Paper

Turbulence-tolerant Manchester On-off Keying Transmission for Free-space Optical Communication

Qian-Wen Jing, Pei-Zheng Yu, Han-Lin Lv, and Yanqing Hong*

School of Information Science and Engineering,
Shenyang University of Technology, Shenyang 110870, China

(Received March 21, 2023 : revised June 14, 2023 : accepted June 21, 2023)

We propose a turbulence-tolerant Manchester on-off keying (M-OOK) transmission for free-space optical (FSO) communication. At the transmitter end, a M-OOK signal featuring a spectrum with low-frequency components absent is modulated and transmitted into a turbulent channel. At the receiver end, a low-pass filter (LPF) -based adaptive-threshold decision (ATD) with LPF-extracted channel-state information (CSI) and a high-pass filter (HPF)-based fixed-threshold decision (FTD) are employed to compensate for the effects of turbulence, owing to the low-frequency spectral characteristics of the turbulent channel. The performance of LPF-based ATD and HPF-based FTD are evaluated for various cutoff frequencies for the LPF and HPF. Besides, the proposed M-OOK transmission is compared to conventional non-return-to-zero OOK (NRZ-OOK) for different data rates. The proposed technique is verified in simulation. The simulation results show that the proposed M-OOK detection with optimized cutoff frequencies of LPF and HPF has better bit-error-rate (BER) performance compared to NRZ-OOK, and it is close to the theoretical ATD with the knowledge of precise CSI under various degrees of turbulence effects.

Keywords : Fixed-threshold decision, Free-space optical communication, High-pass filter, Low-pass filter, Manchester on-off keying
OCIS codes : (010.1330) Atmospheric turbulence; (060.2605) Free-space optical communication; (060.4510) Optical communications

I. INTRODUCTION

Free-space optical (FSO) communication has the features of wide bandwidth, efficient power consumption, low mass, license-free spectrum, and high security compared to conventional radio-frequency (RF) systems [1]. Thus FSO systems have recently attracted dramatic attention as prospective candidates for next-generation wireless communication systems [2]. As to an FSO system, the intensity modulation and direct detection (IM/DD) approach is widely researched, on account of the system's simplicity [3, 4]. Nevertheless, the turbulence-induced scintillation effect leads to significant temporal and spatial fluctuations of the received optical intensity due to variations of the atmosphere. Therefore, it is difficult to effectively estimate the decision threshold for the fluctuating intensity signal in IM/DD FSO systems [5].

Many studies have been conducted to optimize the decision threshold for IM/DD FSO links. A cascaded optical pre-amplifier has been deployed before the photodiode (PD) to accomplish fixed-threshold decision (FTD) via scintillation mitigation, using gain saturation from the optical amplifier [6]. However, the application of a cascaded optical amplifier increases the payload at the receiver end. An avalanche photodiode (APD) has been applied to achieve FTD by input-power-dependent nonlinear optical gain

*Corresponding author: hongy7@sut.edu.cn, ORCID 0000-0002-8460-085X

Color versions of one or more of the figures in this paper are available online.

pISSN: 2508-7266 / eISSN: 2508-7274 https://doi.org/10.3807/COPP.2023.7.4.345

[7]. Whereas the performance of APD is limited to a very weakly turbulent channel, adaptive transmission has been studied to compensate for intensity fluctuation by altering the modulation formats or transmitted optical powers, according to the knowledge of channel-state information (CSI) [8]. Nevertheless, the feedback of CSI from the receiver end is required. A pilot tone and symbol have been introduced to estimate the instantaneous CSI of the turbulent channel from assistant pilot tones or symbols, to realize an adaptive-threshold decision (ATD) [9]. However, the application of pilot tones and symbols increases the system's redundancy and complexity. A low-pass filter (LPF) has been researched to filter out the instantaneous CSI due to the low-frequency spectral characteristics of the turbulent channel [10], but the performance of ATD is decreased in the case of low-speed transmission, due to the serious signal distortion from the LPF. Therefore, Manchester on-off keying (M-OOK), featuring the absence of low-frequency components from the spectrum, is studied to improve the efficiency of decision-threshold estimation.

In this paper, we propose turbulence-tolerant M-OOK transmission for FSO communication. M-OOK modulation is adopted in the transmitter terminal. With regard to the receiver terminal, the M-OOK signal is detected using LPF-based ATD and high-pass filter (HPF)-based FTD, due to the low-frequency spectral characteristics of the turbulent channel. LPF-based ATD and HPF-based FTD are analyzed for different cutoff frequencies of the LPF and HPF. Furthermore, the performance of M-OOK transmission is compared to that of conventional NRZ-OOK for various data rates. The proposed method is evaluated via simulation for various turbulence strengths. The simulation results demonstrate that the bit-error rate (BER) of the proposed M-OOK detection with optimized cutoff frequencies of LPF and HPF shows better performance than in conventional NRZ-OOK, and is close to the theoretical ATD with the knowledge of precise CSI.

II. PRINCIPLE OF OPERATION

Figure 1 shows the block diagram of the proposed M-OOK transmission in FSO communication. The Manchester-encoded OOK signal is directly modulated into a laser diode (LD) with a wavelength of 1,550 nm, and on-to-off and off-to-on represent bits 1 and 0 of the M-OOK signal respectively. Figures 2(a) and 2(b) show the spectra of NRZ-OOK and M-OOK respectively. The M-OOK signal has the features of low-frequency components being absent from the spectrum, compared to NRZ-OOK; However, a larger bandwidth is required for M-OOK signal transmission. When the modulated M-OOK signal travels through the turbulent atmospheric channel, the optical signal suf-

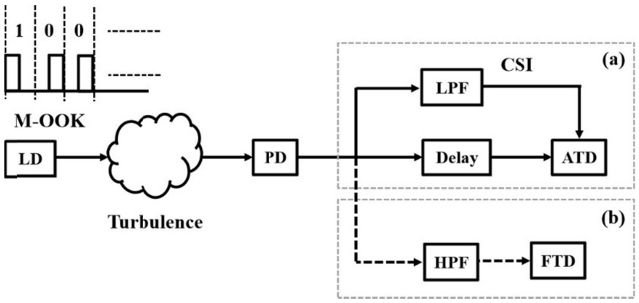

FIG. 1. Block diagram of the proposed technique: (a) LPF-based ATD, (b) HPF-based FTD. LD, laser diode; LPF, low-pass filter; ATD, adaptive-threshold decision; HPF, high-pass filter.

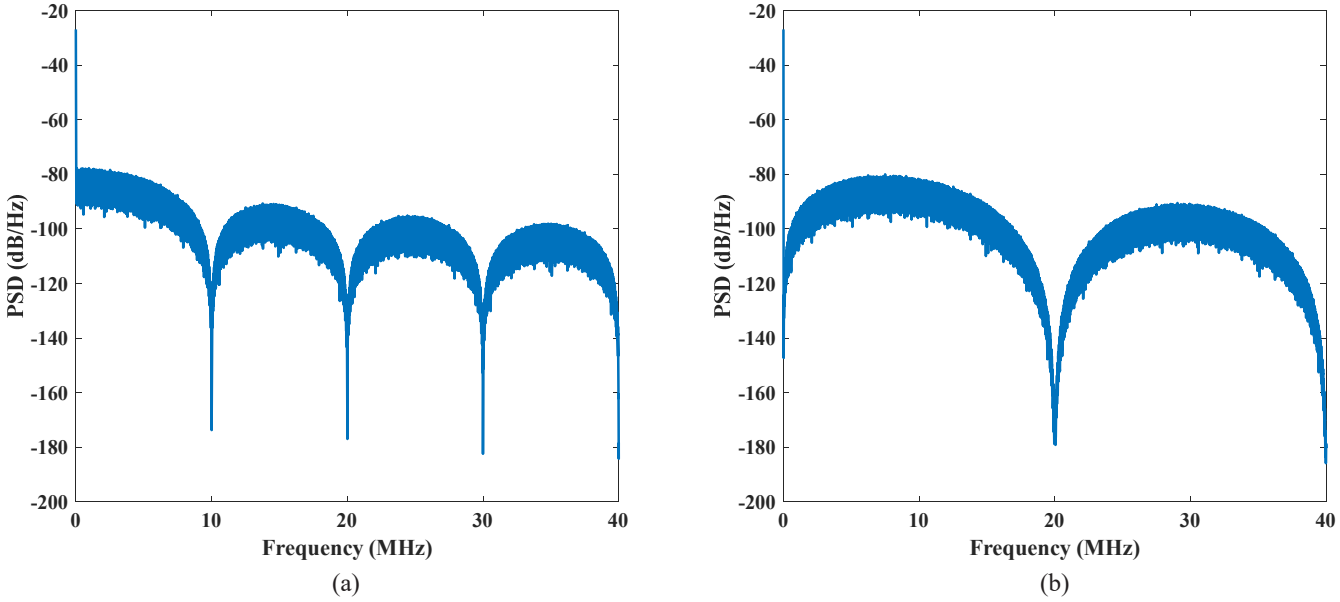

FIG. 2. Spectrum of (a) non-return-to-zero on-off keying (NRZ-OOK), and (b) Manchester OOK (M-OOK).

fers the turbulence effect by reason of randomly varying temperature and pressure of the atmosphere [1]. The turbulence-caused scintillation effect gives rise to the fluctuation of the received signal intensity, as illustrated in Fig. 3(a). The strength of the scintillation effect is measured in terms of the scintillation index σ_I^2. A higher σ_I^2 value indicates a larger degree of intensity fluctuation. σ_I^2 is given by

$$\sigma_I^2 = \left\langle I^2 \right\rangle \Big/ \left\langle I \right\rangle^2 - 1, \tag{1}$$

where I is the signal intensity and $\langle \bullet \rangle$ is the ensemble average [1].

To compensate for the scintillation-caused signal-intensity fluctuation, LPF-based ATD, and HPF-based FTD are introduced to distinguish the bits 1 and 0 of the received M-OOK signal. With respect to M-OOK detection using LPF-based ATD, the received M-OOK signal is equally split into two branches. The upper branch is used to obtain real-time CSI knowledge of the turbulent channel, since the turbulent channel has the characteristics of a low-frequency-dominant spectrum, as shown in Fig. 3(b). Besides, the intensity of the LPF-extracted CSI signal is approximately half of the signal before LPF filtering. Thus, the extracted CSI signal is used directly as a decision threshold for the lower branch's detected M-OOK signal. The delay is used to match the synchronization between upper- and lower-branch signals. Figure 4 shows the spectra of the received NRZ-OOK and M-OOK signals, before and after the turbulent channel. The low-frequency CSI components can be much more effectively extracted from the received M-OOK signal using the cutoff-frequency-optimized LPF, and the LPF-induced signal distortion of M-OOK is reduced, compared to NRZ-OOK, due to the characteristic absence of low-frequency components in the M-OOK signal. With respect to M-OOK detection using HPF-based FTD, the HPF is utilized to block the scintillation effect when low-frequency components dominate the spectral features. Therefore, fixed-threshold estimation is feasible for distinguishing the bits 1 and 0 of the M-OOK signal. Figure 5 depicts the histograms of the NRZ-OOK and M-OOK signals, before and after HPF. The overlapping bits 1 and 0 are effectively separated by HPF, owing to the low-frequency characteristics of the turbulent channel, and the signal distortion from the HPF is significantly reduced. Figure 6 shows the intensity variation of the M-OOK signal before and after HPF. It is obvious that FTD is available for the received M-OOK, signal with the assistance of an HPF. Consequently, the M-OOK signal is effectively detected using LPF-based ATD and HPF-based FTD techniques in a turbulent channel.

III. CHANNEL ANALYSIS

Atmospheric turbulence effects include beam wandering, beam spreading, and beam scintillation. Among these, the scintillation effect causes dramatic temporal and spatial variations of the received signal intensity. Thus it is one of the critical issues of an IM/DD FSO system. In this study, we focus on the scintillation-induced performance degradation for an FSO system. The scintillation effect is modeled using the lognormal distribution, which is a simple and popular model for a weakly turbulent channel. The probability density function (PDF) is calculated by

$$f(I) = 1\Big/\sqrt{2\pi\sigma_I^2 I}\,\exp\left[-\left(\ln(I)-\mu\right)^2\Big/\left(2\sigma_I^2\right)\right], \tag{2}$$

where μ is the mean of $\ln(I)$ [1]. The turbulent channel with the characteristics of time-varying intensity fluctuations is modeled by the process of phase modulation, inverse

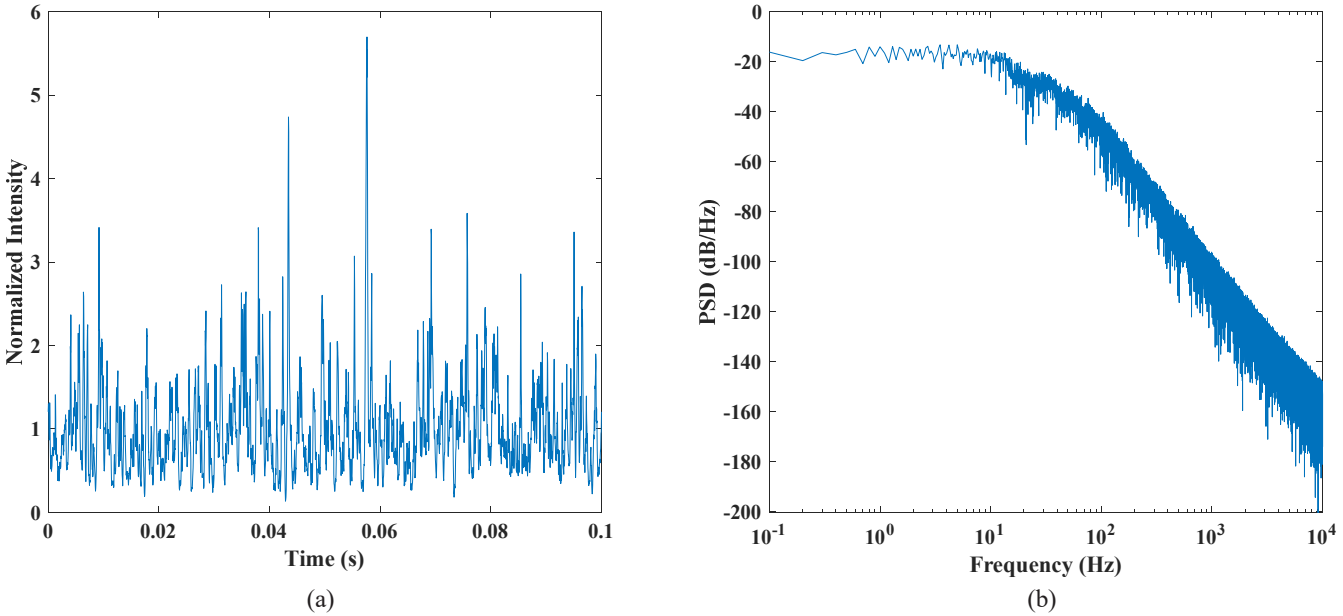

(a) (b)

FIG. 3. Turbulent channel with $\sigma_I^2 = 0.3299$: (a) Intensity fluctuation, (b) spectrum.

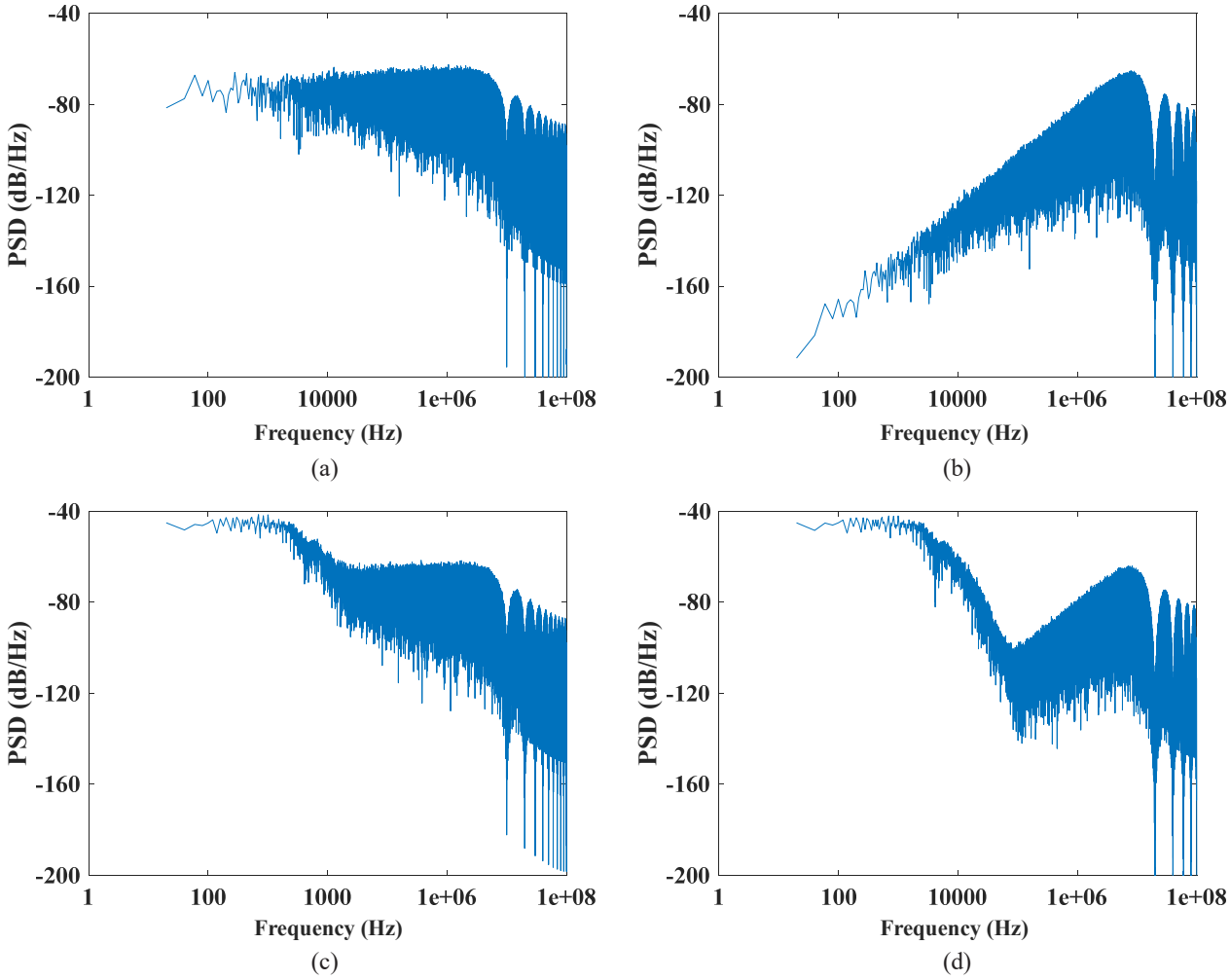

FIG. 4. Spectra of (a) non-return-to-zero on-off keying (NRZ-OOK) before, (b) Manchester OOK (M-OOK) before, (c) NRZ-OOK after, and (d) M-OOK after the turbulent channel.

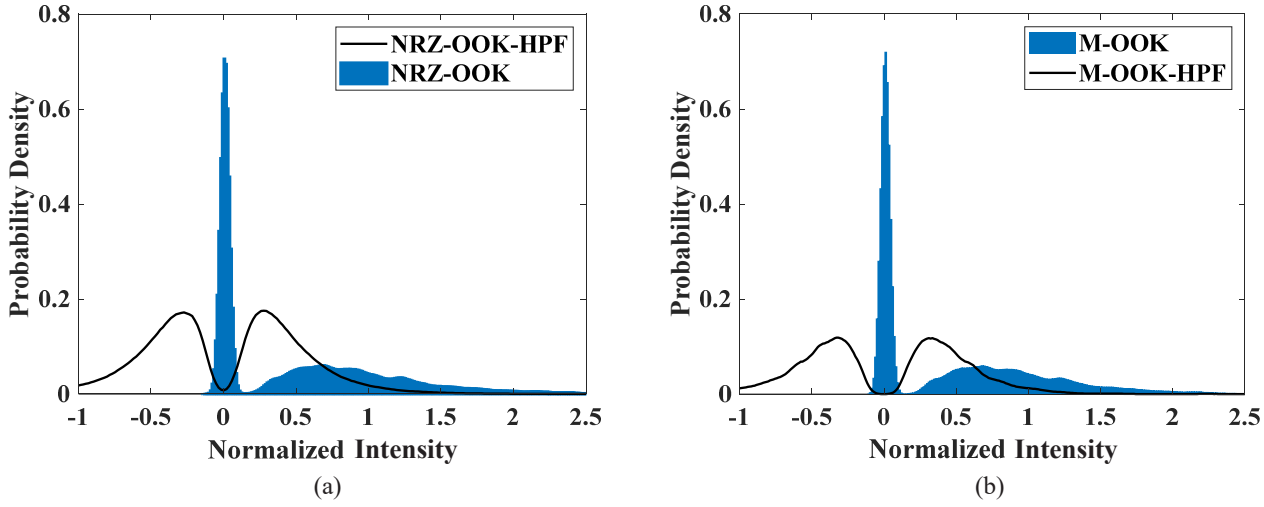

FIG. 5. Comparison of histograms before and after high-pass filter (HPF): (a) Non-return-to-zero on-off keying (NRZ-OOK), (b) Manchester OOK (M-OOK).

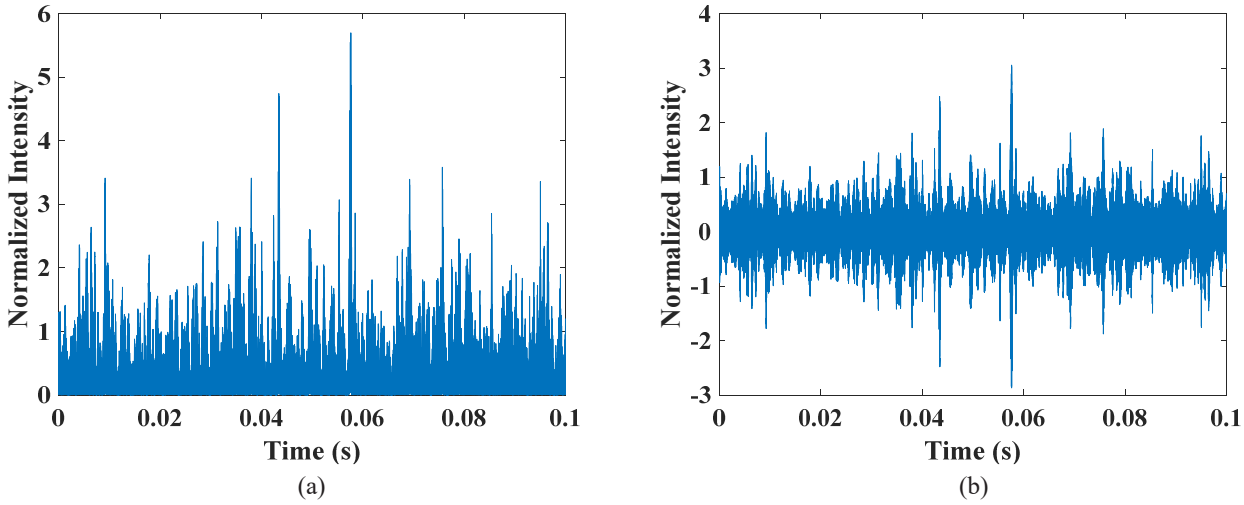

FIG. 6. Intensity variation of the Manchester on-off keying (M-OOK) signal, (a) before and (b) after high-pass filter (HPF).

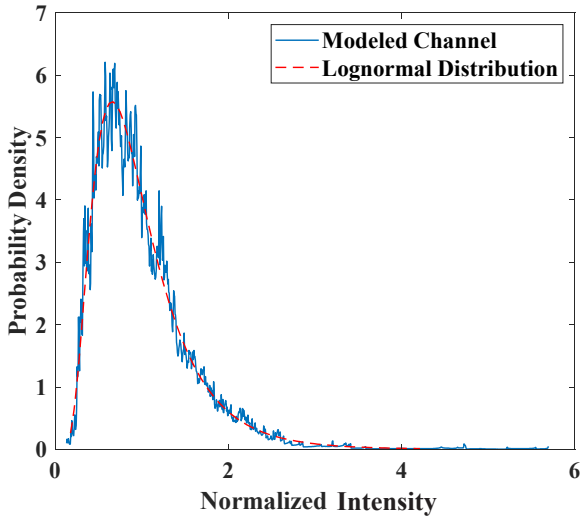

FIG. 7. Comparison of the modeled turbulent channel to a lognormal distribution.

Fourier transform, and first-order Rytov approximation of the temporal spectrum of log-amplitude fluctuations [11]. Figure 7 shows the PDF of the modeled turbulent channel using the parameters from Table 1. The curve of the modeled turbulent channel fits well with the lognormal distribution with $\sigma_I^2 = 0.3299$. The model turbulent channel has the features of time-varying signal intensity [as shown in Fig. 3(a)] and a low-frequency-dominant spectrum [as shown in Fig. 3(b)]. Therefore, it is feasible to accommodate the turbulent channel in the following simulation study.

IV. SIMULATIONS AND RESULTS

The proposed M-OOK detection using LPF-based ATD and HPF-based FTD are evaluated in simulation. The proposed method is compared to NRZ-OOK detection for various cutoff frequencies of LPF and HPF, data rates, and

TABLE 1. Parameters of the turbulent channel

Parameter	Value
Link Distance (km)	10
Wavelength (nm)	1,550
Aperture Diameter (cm)	10
C_n^2	1.5×10^{-11}
Wind Velocity (m/s)	5
Divergence Angle (μrad)	10
Visibility (km)	30

turbulence effects. Figure 8 demonstrates the BER performance of the proposed M-OOK detection for various cutoff frequencies of LPF and HPF. Turbulent channels with $\sigma_I^2 =$ 0.3299 and 0.6789 are adopted in the simulations. The data rates of M-OOK and NRZ-OOK are fixed to 100 Mbps. The average signal-to-noise ratio (SNR) is set to 28 dB, to reduce the impact from the PD and background noises. For M-OOK detection, the range of cutoff frequencies of LPF and HPF are set to 10 Hz–2 MHz and 10 Hz–0.1 MHz respectively. For NRZ-OOK detection, the range of cutoff frequencies of LPF and HPF are set to 10 Hz–0.15 MHz and 10 Hz–0.008 MHz respectively. The reason is that the turbulent channel has a spectrum dominated by low frequencies. The LPF and HPF have wider ranges of cutoff frequencies in the case of M-OOK signal transmission compared to NRZ-OOK, since the M-OOK signal has a spectrum with low-frequency components absent. Besides, the correlation coefficient of the LPF-extracted CSI under M-OOK signal transmission is higher than that for NRZ-OOK. The BER of the proposed M-OOK detection is initially improved by the increase of the cutoff frequencies of LPF and HPF, because the accuracy of CSI estimation was improved for LPF-based ATD, and the degree of scintillation mitigation is increased by HPF-based FTD. However, when the

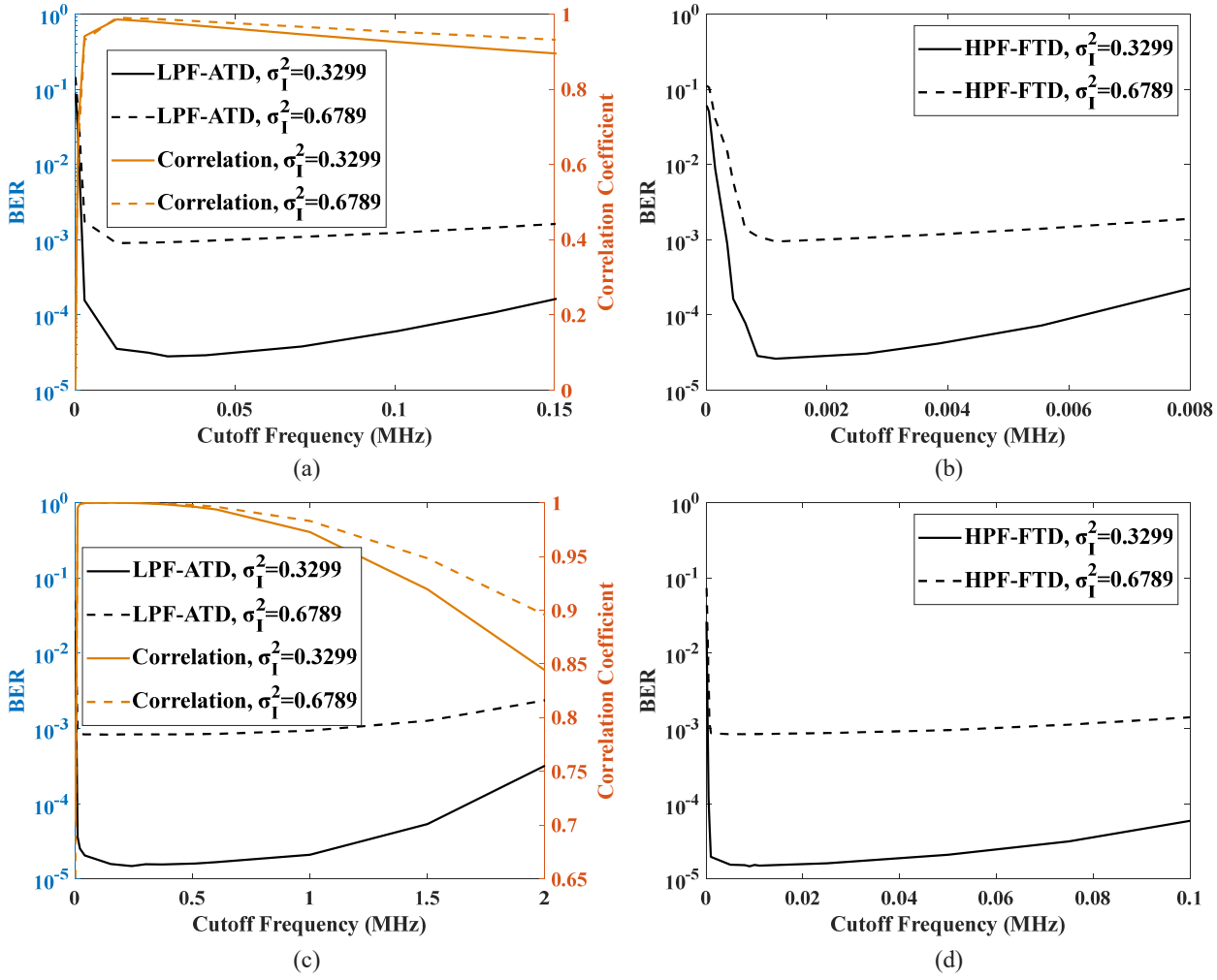

FIG. 8. BER performance of (a) NRZ-OOK with LPF-based ATD and correlation coefficient between LPF-estimated CSI and ideal CSI, (b) NRZ-OOK with HPF-based FTD, (c) M-OOK with LPF-based ATD and correlation coefficient between LPF-estimated CSI and ideal CSI, and (d) M-OOK with HPF-based FTD, at a data rate of 100 Mbps under various cutoff frequencies of LPF, cutoff frequencies of HPF, and σ_I^2. BER, bit-error-rate; NRZ-OOK, non-return-to-zero on-off keying; LPF, low-pass filter; ATD, adaptive-threshold decision; CSI, channel-state information; HPF, high-pass filter; FTD, fixed-threshold decision.

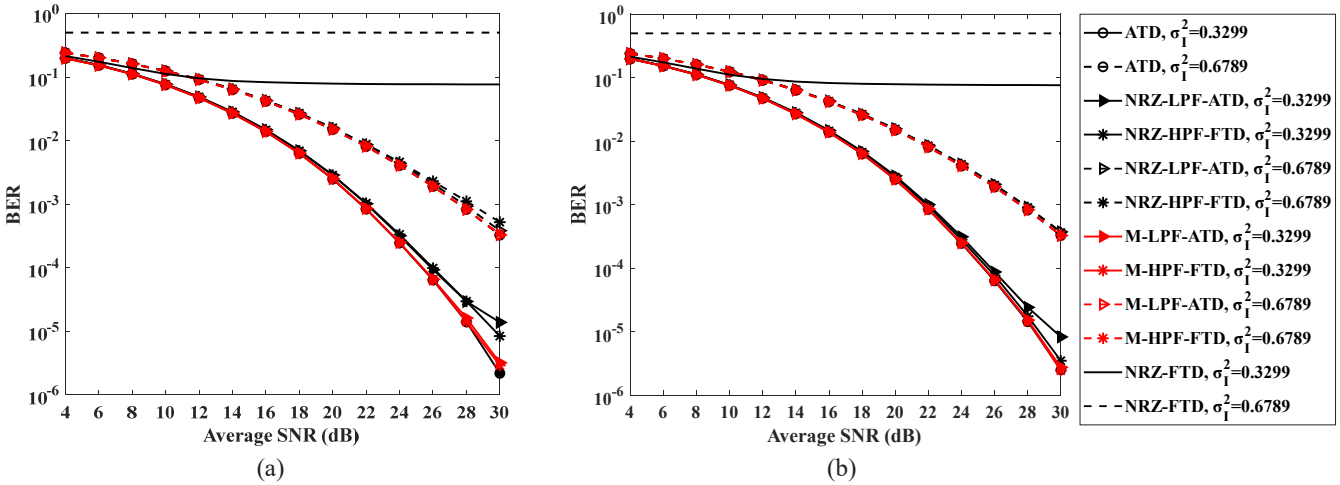

FIG. 9. BER performance of M-OOK and NRZ-OOK detection for various data rates: (a) 100 Mbps, (b) 200 Mbps. ATD, adaptivethreshold decision; NRZ-LPH-ATD, NRZ-OOK detection using LPF-based ATD; NRZ-HPH-FTD, NRZ-OOK detection using HPF-based FTD; M-LPH-ATD, M-OOK detection using LPF-based ATD; M-HPH-FTD, M-OOK detection using HPF-based FTD; M-FTD, NRZ-OOK detection using FTD.

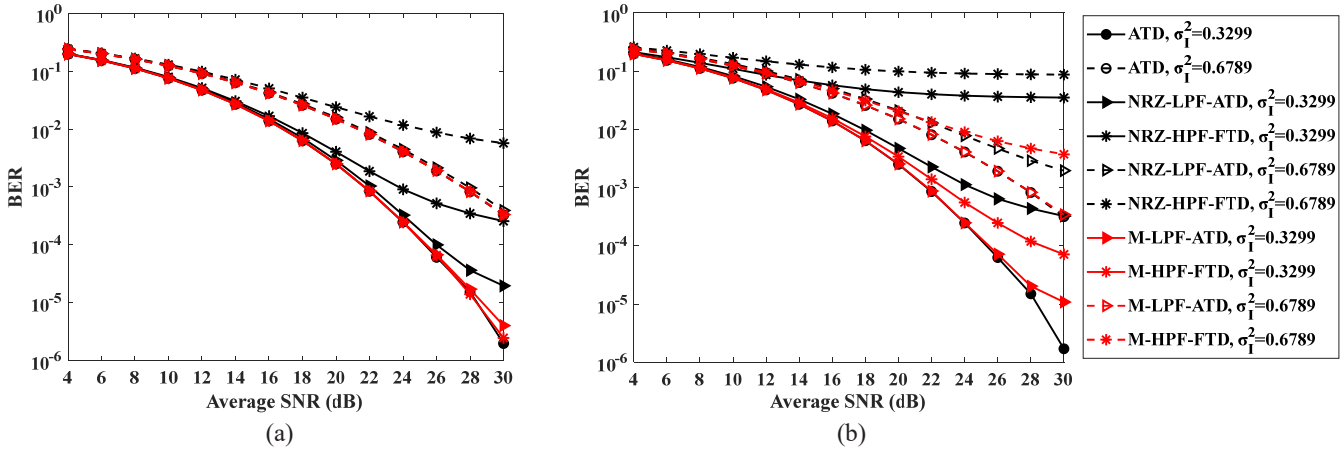

FIG. 10. BER performance of M-OOK and NRZ-OOK detection for various data rates: (a) 50 Mbps, (b) 10 Mbps. BER, bit-error-rate; M-OOK, Manchester on-off keying; NRZ-OOK, non-return-to-zero OOK.

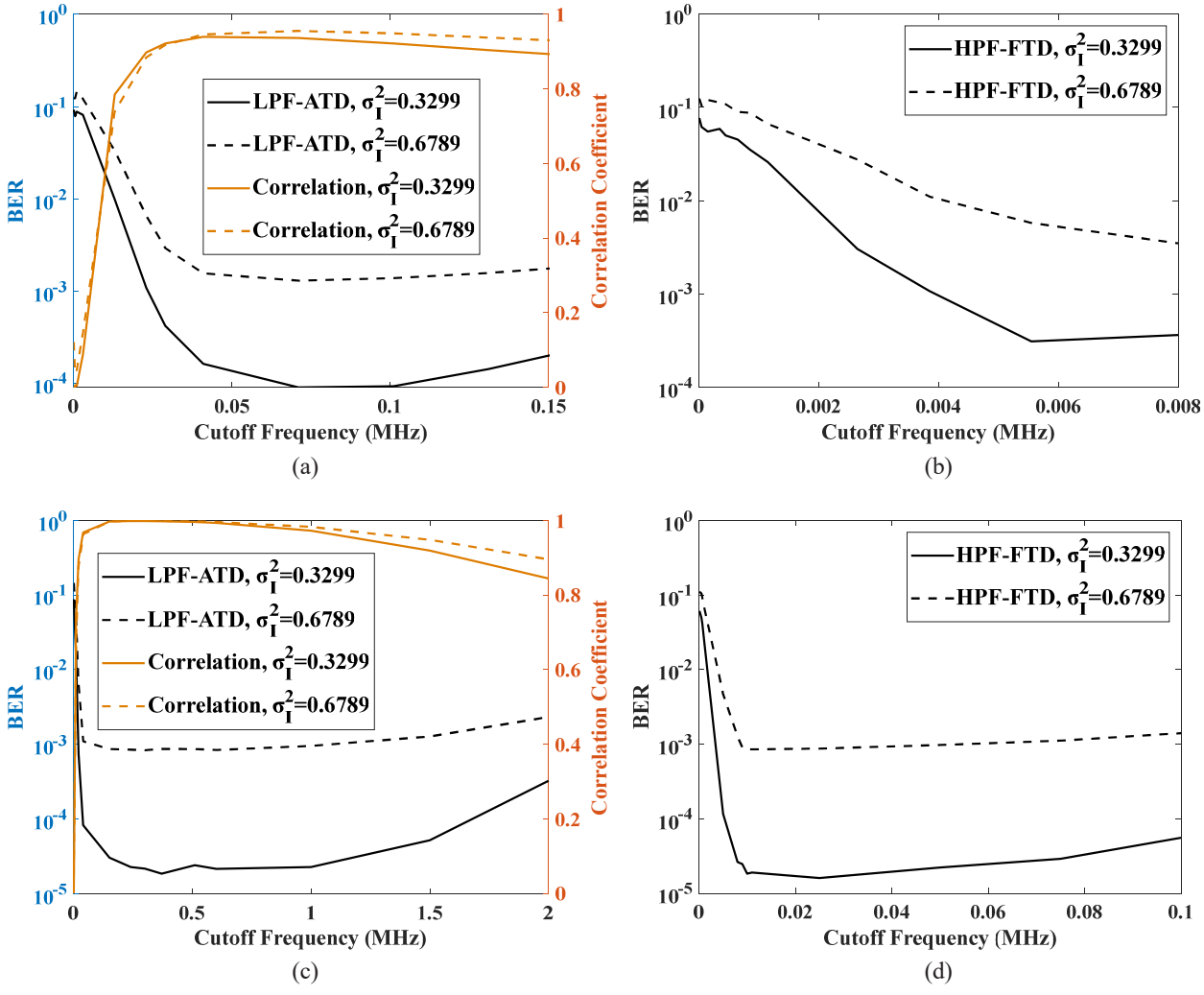

FIG. 11. BER performance of (a) NRZ-OOK with LPF-based ATD and correlation coefficient between LPF-estimated CSI and ideal CSI, (b) NRZ-OOK with HPF-based FTD, (c) M-OOK with LPF-based ATD and correlation coefficient between LPF-estimated CSI and ideal CSI, and (d) M-OOK with HPF-based FTD, at a data rate of 10 Mbps, for various cutoff frequencies of LPF, cutoff frequencies of HPF, and σ_I^2. BER, bit-error-rate; NRZ-OOK, non-return-to-zero OOK; LPD, low-pass filte; ATD, adaptivethreshold decision; CSI, channel-state information; HPF, high-pass filter; FTD, fixed-threshold decision; M-OOK, Manchester on-off keying.

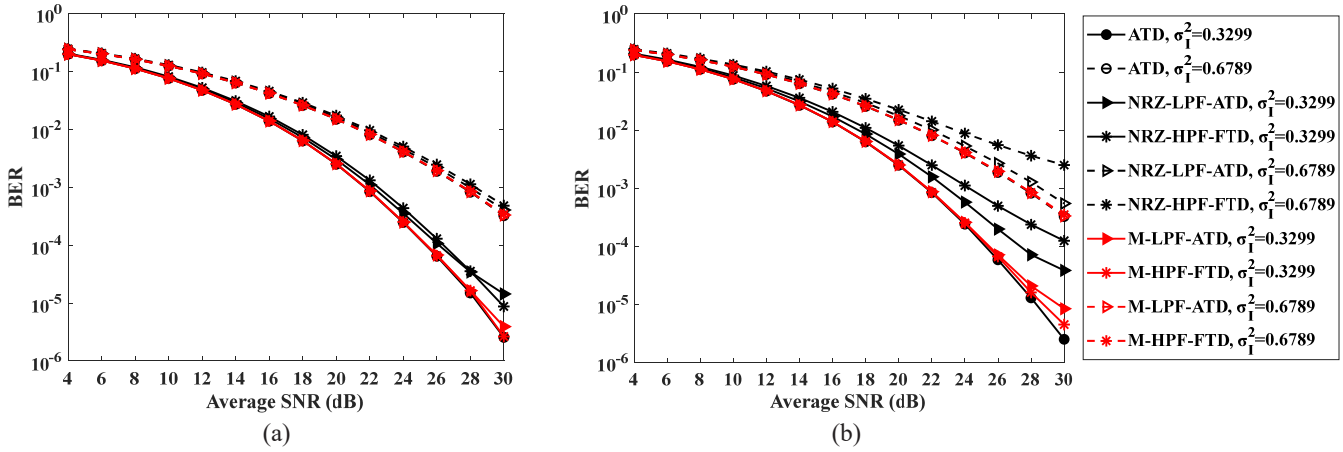

FIG. 12. BER performance of M-OOK and NRZ-OOK detection with optimized cutoff frequencies: (a) 50 Mbps, (b) 10 Mbps. BER, bit-error-rate; M-OOK, Manchester on-off keying; NRZ-OOK, non-return-to-zero OOK.

cutoff frequencies of LPF and HPF exceed critical values, the BER degrades, owing to excessive signal-component extraction and serious signal distortion. Therefore, the proposed M-OOK detection can be realized using optimized cutoff frequencies of LPF and HPF for various σ_I^2.

Figures 9 and 10 depict the BER performance of M-OOK and NRZ-OOK detection using LPF-based ATD and HPF-based FTD, for various data rates. According to Fig. 8, NRZ-OOK with LPF-based ATD, NRZ-OOK with HPF-based FTD, M-OOK with LPF-based ATD, and M-OOK with HPF-based FTD show good BERs for cutoff frequencies of 30 KHz, 1 KHz, 0.30 MHz, and 5 KHz respectively. Thus the cutoff frequencies of the filters are set to these values for LPF and HPF. Regarding NRZ-OOK detection using FTD, it is impossible to distinguish bit values 1 and 0 of the NRZ-OOK signal using a fixed threshold, due to the signal-intensity fluctuation caused by the scintillation effect. With respect to the proposed M-OOK detection for a data rate of 100 Mbps, BER performance similar to the theoretical ATD is observed. Besides, improved BERs are obtained compared to M-OOK detection using FTD, and enhanced BERs are realized compared to NRZ-OOK detection using LPF-based ATD and HPF-based FTD for different SNRs and σ_I^2. The BERs of both M-OOK and NRZ-OOK detection are improved for a data rate of 200 Mbps, due to reduced signal-component extraction by the LPF and signal distortion by the HPF. However, the BER performance is reduced with decreasing data rate, owing to the decreased accuracy of CSI and serious signal distortion from the HPF.

Figure 11 illustrates the BER performance of the proposed M-OOK detection at a data rate of 10 Mbps, for various cutoff frequencies of LPF and HPF. On the basis of Fig. 11, the cutoff frequencies of NRZ-OOK with LPF-based ATD, NRZ-OOK with HPF-based FTD, M-OOK with LPF-based ATD, and M-OOK with HPF-based FTD are optimized to 80 KHz, 6 KHz, 0.37 MHz, and 11 KHz respectively. Figure 12 shows the BER performance of M-OOK and NRZ-OOK detection using LPF-based ATD and HPF-based FTD with optimized cutoff frequencies. The proposed M-OOK detection has better BER performance than NRZ-OOK, due to the absence of low-frequency components in the spectrum of M-OOK. Besides, the BER performance is close to the theoretical ATD for both LPF-based ATD and HPF-based FTD with optimized cutoff frequencies, for data rates of 50 and 10 Mbps. Consequently, the turbulence effect is effectively mitigated by the proposed technique with optimized cutoff frequency, for various data rates and turbulence effects. However, the proposed technique will be ineffective for ultralow-speed M-OOK transmission, due to the cutoff-frequency limitations of LPF and HPF. Besides, LPF and HPF can introduce noises into the LPF-extracted CSI and HPF-filtered M-OOK signals, which will be discussed in further works.

V. CONCLUSIONS

In summary, M-OOK detection using LPF-based ATD and HPF-based FTD was proposed to compensate for the effects of turbulence in FSO communication. The proposed M-OOK detection was analyzed for different cutoff frequencies of LPF and HPF. Besides, the proposed method was compared to NRZ-OOK detection using LPF-based ATD and HPF-based FTD for various data rates. Furthermore, it was compared to the theoretical ATD with the knowledge of precise CSI for various degrees of turbulence. The proposed technique was verified in simulation. The simulation results demonstrated that the BER performance of the proposed technique with optimized cutoff frequency is close to the theoretical ATD; therefore, it is a highly potent and feasible technique for IM/DD FSO systems.

FUNDING

Major Scientific and Technological Innovation Project of Shandong Province (2019JZZY010128); Natural Science

Foundation of Liaoning Province (20180520022).

DISCLOSURES

The authors declare no conflict of interest.

DATA AVAILABILITY

Data underlying the results presented in this paper are not publicly available at this time, but may be obtained from the authors upon reasonable request.

REFERENCES

1. H. Kaushal and G. Kaddoum, "Optical communication in space: Challenges and mitigation techniques," IEEE Commun. Surv. Tutor. **19**, 57–96 (2017).
2. A. S. Hamza, J. S. Deogun, and D. R. Alexander, "Classification framework for free space optical communication links and systems," IEEE Commun. Surv. Tutor. **21**, 1346–1382 (2019).
3. M. A. Khalighi and M. Uysal, "Survey on free space optical communication: a communication theory perspective," IEEE Commun. Surveys Tuts. **16**, 2231–2258 (2014).
4. H. Kaushal, V. K. Jain, and S. Kar, *Free Space Optical Communication* (Springer New Delhi, India, 2017).
5. K. Yoshisada, T. Morio, T. Yoshihisa, and T. Hideki, "The uplink data received by OICETS," J. Nat. Inst. Inform. Commun. Technol. **59**, 117–123 (2012).
6. K. Yiannopoulos, N. C. Sagias, and A. C. Boucouvalas, "Fade mitigation based on semiconductor optical amplifiers," J. Lightw. Technol. **31**, 3621–3630 (2013).
7. X. Yu, L. Xiao, S. Gao, Y. Song, L. Zhang, H. Yao, T. Wang, X. Chen, Z. Jin, C. Zhou, and C. Zhou, "Atmospheric turbulence suppression algorithm based on APD adaptive gain control for FSO links of 5G floating base stations," IEEE Photonics J. **12**, 7904011 (2020).
8. H. Safi, A. A. Sharifi, M. T. Dabiri, I. S. Ansari, and J. Cheng, "Adaptive channel coding and power control for practical FSO communication systems under channel estimation error," IEEE Trans. Veh. Technol. **68**, 7566–7577 (2019).
9. I.-Y. Choi, W.-H. Shin, and S.-K. Han, "CSI estimation with pilot tone for scintillation effects mitigation on satellite optical communication," Opt. Commun. **435**, 88–92 (2019).
10. S. L. Ding, J. K. Zhang, and A. H. Dang, "Adaptive threshold decision for on-off keying transmission systems in atmospheric turbulence," Opt. Express **25**, 24425–24436 (2017).
11. M. Toyoshima, H. Takenaka, and Y. Takayama, "Atmospheric turbulence-induced fading channel model for space-to-ground laser communications links," Opt. Express **19**, 15966–15975 (2011).